Audio Engineering Society

Convention Paper

Presented at the 125th Convention
2008 October 2–5 San Francisco, CA, USA

A Comparison of Wave Field Synthesis and Higher-Order Ambisonics with Respect to Physical Properties and Spatial Sampling

Sascha Spors and Jens Ahrens

Deutsche Telekom Laboratories, Technische Universität Berlin, Ernst-Reuter-Platz 7, 10587 Berlin, Germany

Correspondence should be addressed to Sascha Spors (Sascha.Spors@telekom.de)

ABSTRACT

Wave field synthesis (WFS) and higher-order Ambisonics (HOA) are two high-resolution spatial sound reproduction techniques aiming at overcoming some of the limitations of stereophonic reproduction techniques. In the past, the theoretical foundations of WFS and HOA have been formulated in a quite different fashion. Although, some work has been published that aims at comparing both approaches their similarities and differences are not well documented. This paper formulates the theory of both approaches in a common framework, highlights the different assumptions made to derive the driving functions and the resulting physical properties of the reproduced wave field. Special attention will be drawn to the consequences of spatial sampling since both approaches differ significantly here.

1. INTRODUCTION

Loudspeaker based sound reproduction systems with a high number of reproduction channels are increasingly being proposed and implemented. Typically, the aim of increasing the number of channels, compared e. g. to the nowadays widely used five channels, is to provide high-resolution spatial audio for a potentially large audience. While some of the proposed systems are more or less extensions of stereophonic techniques, others are based on the concept of physically recreating a sound field. Two established approaches of the latter category are wave field synthesis (WFS) and Ambisonics. WFS has initially been proposed by [1] and since then quite a number of systems with some tens to hundreds of reproduction channels have been realized. The term Ambisonics is associated with a variety of approaches. Traditional Ambisonics [2] uses four loudspeakers driven by amplitude panning. It is therefore more an alternative approach to five-channel surround than

a high-resolution replacement. However, the traditional Ambisonics has been extended in various ways. Higher-order Ambisonics (HOA) [3, 4] can use an arbitrary number of reproduction channels and potentially provides a high spatial resolution.
The aim of this paper is to compare the properties of WFS and HOA. The theoretical foundations of WFS and HOA look quite different in their original formulations. While WFS is based on the Kirchhoff-Helmholtz integral, HOA is typically derived on basis of the mode matching approach. A straightforward comparison of the physical properties is therefore difficult. Some work has been published in the past that compares both approaches [5, 6, 7]. These comparisons are based on a spatially continuous formulation of WFS and a spatially discrete formulation of HOA. As a consequence, the influence of spatial sampling could not be formulated analytically and was investigated only by numerical simulations of the reproduced wave field. This paper formulates both approaches in a continuous domain and performs the spatial sampling at a later stage. For this purpose, a common theoretical framework is introduced fostering the comparison of both approaches in more detail as compared to the previous publications.
We begin the paper with a general formulation of the underlying physical problem of sound reproduction in Section 2. Then this theory is applied in order to briefly review the concepts of WFS and HOA in Section 3. A unified formulation of both approaches is furthermore provided ibidem. At the current stage, HOA is limited to circular/spherical loudspeaker arrangements. Therefore, explicit formulations for the reproduced wave fields, the driving functions and spatial sampling are derived in Section 4 for circular WFS and HOA systems. The theory developed so far, lays then the fundament for a detailed comparison of both approaches in Section 5.

2. BASIC THEORY

This section introduces the basic theory of sound field reproduction. This serves as basis for the derivation of WFS and HOA given in the next section.

2.1. The Kirchhoff-Helmholtz Integral

A loudspeaker system surrounding the listener can be regarded as an inhomogeneous boundary condition. The solution of the homogeneous wave equation for a bounded region V with respect to inhomogeneous boundary conditions is given by the Kirchhoff-Helmholtz integral [8]

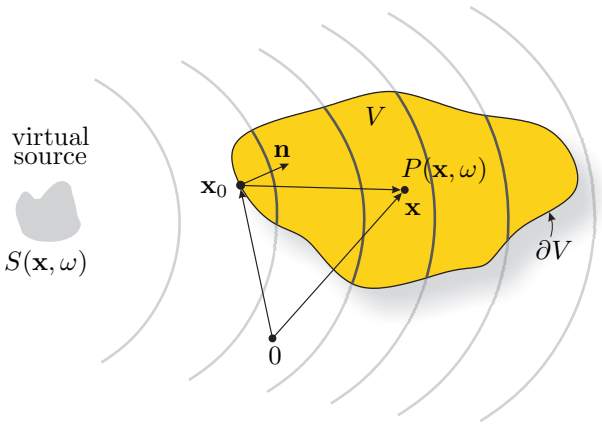

Fig. 1: Illustration of the geometry used for the Kirchhoff-Helmholtz integral (1).

$$P(\mathbf{x},\omega) = -\oint_{\partial V} \left(G(\mathbf{x}|\mathbf{x}_0,\omega)\, \frac{\partial}{\partial \mathbf{n}} P(\mathbf{x}_0,\omega) - P(\mathbf{x}_0,\omega)\, \frac{\partial}{\partial \mathbf{n}} G(\mathbf{x}|\mathbf{x}_0,\omega) \right) dS_0 \;, \quad (1)$$

where $P(\mathbf{x},\omega)$ denotes the pressure field inside a bounded region V enclosed by the boundary ∂V ($\mathbf{x} \in V$), $G(\mathbf{x}|\mathbf{x}_0,\omega)$ a suitably chosen Green's function, $P(\mathbf{x}_0,\omega)$ the acoustic pressure at the boundary ∂V ($\mathbf{x}_0 \in \partial V$) and $\mathbf{n}$ the inward pointing normal vector of ∂V. The abbreviation $\frac{\partial}{\partial \mathbf{n}}$ denotes the directional gradient in direction of the normal vector $\mathbf{n}$. The wave field $P(\mathbf{x},\omega)$ outside of V is zero and V is assumed to be source-free. Figure 1 illustrates the geometry. For sound reproduction typically free-field propagation within V is assumed. This implies that V is free of any objects and that the boundary ∂V does not restrict propagation. The Green's function is then given as the free-field solution of the wave equation and is referred to as *free-field Green's function* $G_0(\mathbf{x}|\mathbf{x}_0,\omega)$. The free-field Green's function can be interpreted as the spatio-temporal transfer function of a monopole placed at the point $\mathbf{x}_0$ and its directional gradient as the spatio-temporal transfer function of a dipole at the point $\mathbf{x}_0$, whose main axis points towards $\mathbf{n}$.
Equation (1) states that if the Green's function is re-

alized by a continuous distribution of appropriately driven monopole and dipole sources which are placed on the boundary ∂V, the wave field within V is fully determined by these sources. This principle can be used for sound reproduction as will be illustrated in the following. In this context the monopole and dipole sources on the boundary are referred to as (monopole/dipole) *secondary sources*.

The Kirchhoff-Helmholtz integral implies, that authentic sound field reproduction can be realized if a distribution of secondary monopole and dipole sources on the boundary ∂V of the listening area V is driven by the directional gradient and the pressure of the wave field of the virtual source $S(\mathbf{x}, \omega)$, respectively. The Kirchhoff-Helmholtz integral and its interpretation given above lay the theoretical foundation for a variety of massive multichannel sound reproduction systems.

It is desirable for a practical implementation to discard one of the two types of secondary sources. Monopole sources can be realized reasonably well by loudspeakers with closed cabinets. At least two different classes of approaches can be identified to remove the dipole contributions in the Kirchhoff-Helmholtz integral. These are discussed in the following two subsections.

2.2. Neumann Green's Function

The second term in the Kirchhoff-Helmholtz integral (1), representing the dipole secondary sources, can be eliminated by changing the Green's function used in the Kirchhoff-Helmholtz integral [8]. Depending on the situation, this may also imply that other sources than monopoles have to be used as secondary sources.

The basic concept is to use a Neumann Green's function in order to eliminate the dipole secondary sources. A Neumann Green's function has to obey the following condition

$$\frac{\partial}{\partial \mathbf{n}} G_{\mathrm{N}}(\mathbf{x}|\mathbf{x}_0, \omega)\Big|_{\mathbf{x}_0 \in \partial V} = 0 \; . \tag{2}$$

Introducing the definition of the Neumann Green's function (2) into the Kirchhoff-Helmholtz integral (1) yields the reproduced wave field as

$$P(\mathbf{x}, \omega) = - \oint_{\partial V} \frac{\partial}{\partial \mathbf{n}} S(\mathbf{x}_0, \omega)\, G_{\mathrm{N}}(\mathbf{x}|\mathbf{x}_0, \omega)\; dS_0 \; . \tag{3}$$

The explicit form of the Neumann Green's function depends on the geometry of the boundary ∂V. A closed form solution can only be found for rather simple geometries like spheres and planar boundaries [9]. The boundary ∂V is implicitly modeled as an acoustically rigid surface for the secondary sources. This is a consequence of the condition given by Eq. (2).

Equation (3) states, that if the Neumann Green's function can be realized by an physically existing secondary source, then the driving signal is simply given by the directional gradient of the virtual source. Depending on the explicit form of the Neumann Green's function such secondary sources may be impossible to realize in practice.

2.3. Monopole Only Formulation

There are various approaches to derive a monopole only formulation of the Kirchhoff-Helmholtz integral. A direct approach would be to assume monopole only reproduction and to evaluate the properties of the solution. Another approach, which is often considered, is the simple source approach [8, 10]. The simple source approach is derived by constructing an exterior and separately an interior problem with respect to the same boundary ∂V and linking both problems by requiring that the pressure is continuous and the directional gradient is discontinuous at the boundary ∂V.

To the knowledge of the authors, both approaches seem to produce similar results. They result in a monopole only formulation of sound reproduction

$$P(\mathbf{x}, \omega) = \oint_{\partial V} D(\mathbf{x}_0, \omega)\, G_0(\mathbf{x}|\mathbf{x}_0, \omega)\; dS_0 \; . \tag{4}$$

Equation (4) states that a distribution of monopole sources on ∂V driven by $D(\mathbf{x}_0, \omega)$ determines the wave field $P(\mathbf{x}, \omega)$ within and outside of V. Note, that contrary to the Kirchhoff-Helmholtz formulation the wave field outside of V will not be zero in this case. Problems arise at the eigenfrequencies of the interior homogeneous Dirichlet problem [10]. The wave field within V cannot be controlled at these frequencies and is consequently not determined uniquely. This problem is refereed to as non-uniqueness in the following.

The Green's function in Eq. (4) characterizes the field of the secondary sources, the remaining terms their strength. The strength will be termed as

secondary source driving function in the following. An appropriate secondary source driving function $D(\mathbf{x}_0, \omega)$ for a desired virtual wave field can be derived by explicitly solving the integral equation (4) or by applying the simple source approach.

An explicit solution of (4) can be found by applying results from functional analysis, for instance, decomposition of the respective wave fields with respect to orthogonal basis functions. Note, that the underlying problem might be ill-posed.

The simple source approach states that the driving function is given as the difference of the directional gradients when approaching the boundary ∂V from the outside and the inside. Hence, the driving function can be derived by constructing an exterior field that satisfies the required boundary conditions. An appropriate exterior field can be derived by considering the equivalent acoustic scattering problem [11]. Common to all these approaches is, that an explicit formulation of the driving function is only possible by considering special geometries for the secondary source contour ∂V.

In higher-order Ambisonics [3], and other reproduction techniques [12, 13, 14, 15] which are inherently based on the simple source approach, Eq. (4) is explicitly solved with respect to $D(\mathbf{x}_0, \omega)$. For the geometries considered in HOA this is typically performed by expanding the respective wave fields using spherical harmonics or Fourier series.

The monopole only formulation, as presented above, corrects for the missing dipole sources by modifying the driving function. The Neumann Green's function method, as presented in Section 2.2, applies a modified Green's function in order to remove the dipole secondary sources and requires no modification of the driving function. At least in some cases, both methods can be linked directly to each other. For instance, if the Neumann Green's function can be expressed as a multiplication of terms describing a monopole source and other terms. These other terms can then be aggregated to the driving function of the Neumann case. For a spherical secondary source contour this procedure is straightforward when considering e. g. the Rayleigh-like integrals [8].

3. WAVE FIELD SYNTHESIS AND HIGHER-ORDER AMBISONICS

The two concepts to eliminate the dipole secondary sources, introduced in the previous section, are now applied to derive WFS and HOA.

3.1. Wave Field Synthesis

The theory of WFS is based on eliminating the dipole secondary sources by using an appropriate Neumann Green's function. It was already outlined in Section 2.2, that the physical realization of a Neumann Green's function by secondary sources might be impossible for complex secondary source contours ∂V. For a linear/planar secondary source contour the Neumann Green's function takes a form which can be realized straighforwardly by secondary monopole sources. WFS is explicitly based on the Neumann Green's function for a linear/planar boundary. Some extensions to the basic theory are applied, in order to cover curved secondary source contours. The following section outlines the derivation of WFS. A detailed discussion which is based on the same physical framework, as used here, can be found in [16].

A suitable Neumann Green's function for a planar/linear boundary ∂V can be derived by adding an image source with respect to the boundary ∂V to the free-field Green's function [8]. This solution fulfils the condition (2) due to the specialized geometry. In this case the Neumann Green's function is given as

$$G_\mathrm{N}(\mathbf{x}|\mathbf{x}_0, \omega)\Big|_{\mathbf{x}_0 \in \partial V} = 2\, G_0(\mathbf{x}|\mathbf{x}_0, \omega)\,. \qquad (5)$$

Hence, for the linear/planar case $G_\mathrm{N}(\mathbf{x}|\mathbf{x}_0, \omega)$ is equal to a monopole source with double strength. Introducing $G_\mathrm{N}(\mathbf{x}|\mathbf{x}_0, \omega)$ into the Kirchhoff-Helmholtz integral derives the first Rayleigh integral, which is the basis for the traditional derivation of WFS [1]. However, this theoretical basis holds only for linear/planar secondary source distributions. In WFS, it is assumed that Eq. (5) holds also approximately for other geometries. The elimination of the secondary dipole sources for an arbitrary secondary source contour ∂V has two consequences:

1. the wave field outside of V will not be zero, and
2. the reproduced wave field will not match the virtual source field exactly within V.

The first consequence implies that the boundary ∂V has to be convex, so that no contributions from the

wave field outside of the listening area V propagate back into the listening area. The second is a consequence of approximating the Neumann Green's function for arbitrary geometries using (5). Using this Neumann Green's function for curved secondary source contours leads to artifacts in the reproduced wave field. One possibility is to mute those secondary sources whose normal vector $\mathbf{n}$ does not coincide with the local propagation direction of the virtual wave field.
Following this concept, the reproduced wave field reads

$$P(\mathbf{x},\omega) = - \oint_{\partial V} 2a(\mathbf{x}_0) \frac{\partial}{\partial \mathbf{n}} S(\mathbf{x}_0,\omega)\, G_0(\mathbf{x}|\mathbf{x}_0,\omega)\, dS_0 \;, \quad (6)$$

where $a(\mathbf{x}_0)$ denotes a suitably chosen window function. This function takes care that only those secondary sources are active where the local propagation direction of the virtual source at the position $\mathbf{x}_0$ has a positive component in direction of the normal vector $\mathbf{n}$ of the secondary source. It was proposed in [17] to formulate this condition analytically on basis of the acoustic intensity vector.
For an arbitrarily shaped boundary ∂V, the reproduced wave field will not exactly match the virtual source field $S(\mathbf{x},\omega)$ within V. However, this approximation seems to be reasonable for sound reproduction purposes.

3.2. Higher-order Ambisonics

In the literature, several variants of Ambisonics exist. They differ in the assumptions made for the secondary sources and the procedure used to derive the desired virtual wave field. Since the focus of this contribution lies on the comparison of HOA with WFS we will assume model-based reproduction with monopole sources as secondary sources. This variant of Ambisonics is also known as near-field compensated HOA [4]. We will further skip the en-/deconding procedure, typically used in the traditional derivation of HOA, for the sake of clarity. The theory of HOA is often based on the direct assumption of a spatially discrete distribution of secondary sources. However, the analysis of sampling artifacts is simplified by formulating the problem in a continuous domain and introducing the spatial discretization separately.

In this case, the driving function for HOA is derived by explicitly solving the integral equation (4) with respect to the secondary source driving function $D_{\mathrm{HOA}}(\mathbf{x}_0,\omega)$. As outlined above, decomposition of the involved wave fields into orthogonal basis functions is a standard solution applied to integral equations in the form of Eq. (4). The orthogonal expansion of wave fields transforms the integral equation into an equation containing only sums. The resulting equation is then solved by comparison of coefficients or by setting up a linear system of equations. The particular choice of basis functions depends on the secondary source contour and the dimensionality of the problem. In the context of HOA, circular and spherical secondary source contours have been considered so far. A detailed derivation of driving functions for continuous circular/spherical contours can be found in [12, 13, 15]. For a circular geometry exponential functions with respect to the angular coordinate of a polar coordinate systems are suitable (Fourier series), for a spherical geometry spherical harmonics. The explicit form of the driving function for a circular boundary will be derived in Section 4.2.

3.3. Unified Formulation

The following section will develop a unified formulation of WFS and HOA, which will be used for the comparison of both approaches.
This unified formulation is derived straightforwardly by comparing Eq. (4) with Eq. (6). This reveals that the sound pressure $P(\mathbf{x},\omega)$ inside the listening area can be expressed by the secondary source driving function $D(\mathbf{x}_0,\omega)$ and the Green's function $G_0(\mathbf{x}|\mathbf{x}_0,\omega)$ as

$$P(\mathbf{x},\omega) = - \oint_{\partial V} D(\mathbf{x}_0,\omega)\, G_0(\mathbf{x}|\mathbf{x}_0,\omega)\, dS_0 \;. \quad (7)$$

The Green's function characterizes the wave field emitted by the secondary sources. For WFS and HOA these are assumed to be monopoles placed at the boundary ∂V. The explicit form of the Green's function depends on the dimensionality of the problem.
For three-dimensional reproduction this is the field of a point source, for two-dimensional reproduction this is the field of a line source. Sound reproduction in a plane, ideally leveled with the listeners ears, is referred to as two-dimensional reproduction. The required reduction in dimensionality is performed by

assuming that the reproduced wave field is independent from the z-coordinate.
Line sources would be the appropriate choice as secondary sources for two-dimensional reproduction. However, since line sources are hard to realize in practice, point sources are typically used for two-dimensional reproduction. This secondary source type mismatch results in various artifacts for WFS [16, 18] and HOA [12, 13] that can be compensated for only to some extend. The remaining most prominent artifacts are amplitude errors. We will discard setups exhibiting a secondary source type mismatch for the comparison of both approaches.
The secondary source driving function $D(\mathbf{x}_0, \omega)$ plays an important role since it determines the loudspeaker signals in a practical implementation. The secondary source driving function for WFS $D_{\mathrm{WFS}}(\mathbf{x}_0, \omega)$ can be derived from Eq. (6) as

$$D_{\mathrm{WFS}}(\mathbf{x}_0, \omega) = -2a(\mathbf{x}_0)\frac{\partial}{\partial \mathbf{n}} S(\mathbf{x}_0, \omega) \; . \qquad (8)$$

The driving function $D_{\mathrm{HOA}}(\mathbf{x}_0, \omega)$ for HOA depends on the particular geometry of ∂V. An explicit expression will be derived in the next section.

4. REPRODUCTION ON CIRCULAR ARRAYS

Since HOA is based on a circular/spherical secondary source contour, such geometries will be considered for the comparison of both approaches. For the sake of clarity, we will assume two-dimensional reproduction using a circular secondary source contour with line sources as secondary sources for both WFS and HOA. We will follow the framework developed in [19, 7].

4.1. Reproduced Wave Field

The two-dimensional free-field Green's function is given as

$$G_{\mathrm{2D}}(\mathbf{x}|\mathbf{x}_0, \omega) = \frac{j}{4} H_0^{(2)}(\frac{\omega}{c}\,|\mathbf{x} - \mathbf{x}_0|) \; , \qquad (9)$$

where $H_0^{(2)}(\cdot)$ denotes the zeroth-order Hankel function of second kind [20] and $\mathbf{x} = [x\; y]^T$. Equation (9) can be interpreted as the field of a line source. This line source is located parallel to the z-axis and intersects with the reproduction plane at the position $\mathbf{x}_0$. The reproduced wave field for a circular distribution of secondary monopole line sources is given by introducing (9) into (7) for the specialized geometry.

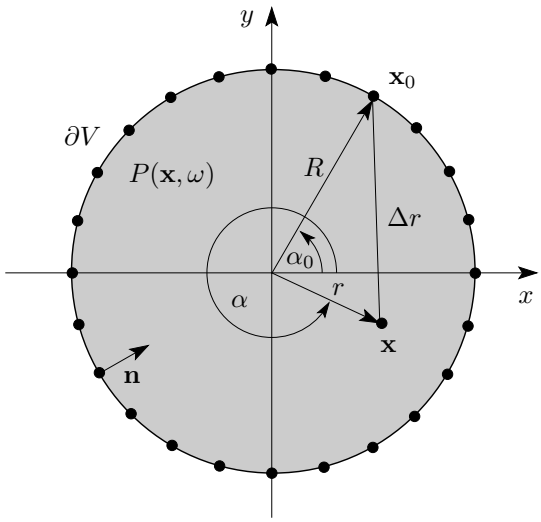

Fig. 2: Geometry used to derive the wave fields reproduced by WFS and HOA. The dots • denote the spatial sampling positions of the secondary sources.

Figure 2 illustrates the geometry. The reproduced wave field $P(\mathbf{x}, \omega)$ reads

$$P(\mathbf{x}, \omega) = -\frac{j}{4} \int_0^{2\pi} D(\alpha_0, R, \omega)\, H_0^{(2)}(k\Delta r)\; R\, d\alpha_0 \; , \qquad (10)$$

where $\Delta r = |\mathbf{x} - \mathbf{x}_0|$. The next step is to express the driving function $D(\alpha_0, R, \omega)$ as Fourier series

$$D(\alpha_0, R, \omega) = \sum_{\nu=-\infty}^{\infty} \mathring{D}(\nu, R, \omega)\, e^{j\nu\alpha} \; , \qquad (11)$$

where $\mathring{D}(\nu, R, \omega)$ denote the Fourier series coefficients of the driving function. Applying the addition theorem for Hankel functions [21] and exploiting the orthogonality of the exponential functions allows to eliminate the angular integral, resulting in

$$P(\mathbf{x}, \omega) = \\ -\, j\frac{\pi}{2} R \sum_{\nu=-\infty}^{\infty} J_\nu(kr)\, H_\nu^{(2)}(kR)\; \mathring{D}(\nu, R, \omega)\, e^{j\nu\alpha} \; . \qquad (12)$$

The variable ν can be interpreted as angular frequency. The representation (12), as sum with respect to the angular frequency, is especially useful in the context of angular sampling. This due to the

fact, that the angular spectrum of the reproduced wave field is given by a multiplication of the angular spectrum of the secondary source spectrum and the driving function.

4.2. Driving Functions

The particular form of the driving function for WFS and HOA depends on the desired virtual wave field to be reproduced. We will consider virtual plane waves for the comparison of both approaches since arbitrary wave fields can be decomposed into plane waves [8].

The HOA driving function for a virtual plane wave with incidence angle θ_{pw} can be derived by equating the right hand side of Eq. (12) with the desired wave field of a plane wave. Expressing a plane wave as Fourier series using the Jacobi-Anger expansion and performing a comparison of the series coefficients yields

$$\mathring{D}_{\mathrm{HOA}}(\nu, R, \omega) = -\frac{2}{j\pi R} \frac{j^{-\nu} J_\nu(kr)}{J_\nu(kR)\, H_\nu^{(2)}(kR)} e^{-j\nu\theta_{\mathrm{pw}}} \; . \tag{13}$$

Note, that the Bessel function in the numerator and denominator of Eq. (13) cannot be canceled straightforwardly to the zeros of the Bessel function. The angular spectrum $\mathring{D}_{\mathrm{WFS}}(\nu, R, \omega)$ of the driving function for WFS cannot be derived as straightforwardly as for HOA, due to the involved window function. The driving function for WFS is given as [16]

$$\begin{aligned} &D_{\mathrm{WFS}}(\alpha_0, R, \omega) = \\ &2j\frac{\omega}{c} a_{\mathrm{pw}}(\alpha_0) \cos(\alpha_0 - \theta_{\mathrm{pw}}) e^{-j\frac{\omega}{c} R \cos(\alpha_0 - \theta_{\mathrm{pw}})} \; , \end{aligned} \tag{14}$$

where the window function for a plane wave $a_{\mathrm{pw}}(\alpha_0) = 1$ for $\cos(\alpha_0 - \theta_{\mathrm{pw}}) > 0$ and zero elsewhere. The Fourier series coefficients $\mathring{D}_{\mathrm{WFS}}(\nu, R, \omega)$ can be computed by performing a Fourier transformation with respect to the angle α_0.

4.3. Spatial Sampling

The discretization of the secondary source distribution is modeled conveniently by sampling of the loudspeaker driving function $D(\alpha_0, R, \omega)$ at N equidistant angles (as illustrated by the black bullets in Fig. 2). Angular sampling results in repetitions of the angular spectrum [19]. The Fourier series coefficients $\mathring{D}_{\mathrm{S}}(\nu, R, \omega)$ of the sampled driving function are given as

$$\mathring{D}_{\mathrm{S}}(\nu, R, \omega) = \sum_{\eta=-\infty}^{\infty} \mathring{D}(\nu + \eta N, R, \omega) \; . \tag{15}$$

Introducing (15) into (12) yields the wave field reproduced by a discrete secondary source distribution.

In HOA, the angular bandwidth of the continuous driving driving function (13) is typically limited as follows

$$\begin{aligned} &\mathring{D}_{HOA,N}(\nu, R, \omega) = \\ &\quad \begin{cases} \mathring{D}_{HOA}(\nu, R, \omega) & , \text{for } |\nu| \leq (N-1)/2 \\ 0 & , \text{otherwise.} \end{cases} \end{aligned} \tag{16}$$

for odd N, analogous for even N. Traditionally this limitation has been applied due to the underlying spatially discrete formulation. However, as shown later, this limitation of the angular bandwidth has also influence on the properties of the reproduced wave field with respect to truncation and spatial sampling artifacts. Truncation artifacts will not be discussed in this paper. Please refer to e. g. [14, 12] for a detailed treatment.

The formulation of the reproduced wave field in terms of angular frequencies given by Eq. (12) and Eq. (15) can be used to investigate the effects of spatial sampling. This is performed by splitting up the reproduced wave field $P_{\mathrm{S}}(\mathbf{x}, \omega)$ into the wave field $P_{\mathrm{S},0}(\mathbf{x}, \omega)$ containing no angular repetitions and $P_{\mathrm{S,al}}(\mathbf{x}, \omega)$ containing all repetitions. The wave field $P_{\mathrm{S},0}(\mathbf{x}, \omega)$ would have been reproduced by a continuous secondary source distribution. It is given as

$$\begin{aligned} &P_{\mathrm{S},0}(\mathbf{x}, \omega) = \\ &-j\frac{\pi}{2} R \sum_{\nu=-\infty}^{\infty} \mathring{D}_{\mathrm{S}}(\nu, R, \omega)\; J_\nu(kr)\, H_\nu^{(2)}(kR)\; e^{j\nu\alpha} \; . \end{aligned} \tag{17}$$

Note, that Eq. (17) inherently includes the truncation artifacts of HOA in the desired wave field. The contributions $P_{\mathrm{S,al}}(\mathbf{x}, \omega)$ reproduced by a spatially discrete secondary source distribution can be derived by considering only the spectral repetitions defined

by Eq. (15)

$$P_{\mathrm{S,al}}(\mathbf{x},\omega) = -j\frac{\pi}{2}R \times$$
$$\times \sum_{|\eta|\geq 1} \sum_{\nu=-\infty}^{\infty} \mathring{D}_{\mathrm{S}}(\nu+\eta N, R, \omega) J_\nu(kr)\, H_\nu^{(2)}(kR)\, e^{j\nu\alpha} \,. \tag{18}$$

The split-up of the reproduced wave field is used to calculate the energy of the contributions due to the spectral repetitions with respect to the desired wave field. The reproduced aliasing-to-signal ratio RASR [19] is defined as follows

$$\mathrm{RASR}(\mathbf{x},\omega) = \frac{\int_0^\omega \left|P_{\mathrm{S,al}}(\mathbf{x},\omega')\right|^2 d\omega'}{\int_0^\omega \left|P_{\mathrm{S},0}(\mathbf{x},\omega')\right|^2 d\omega'} \,. \tag{19}$$

The RASR is a measure for the artifacts due to sampling. The truncation artifacts are explicitly discarded due to the definition of the desired wave field given by (17).

Note, that the psychoacoustic relevance of the RASR is unclear at the current stage and will be investigated further. It will be used, however, due to a lack of alternatives.

The unified formulation of WFS and HOA developed so far, for a circular secondary source distribution, lays the theoretical fundament for the comparison of both approaches.

5. COMPARISON OF THE PROPERTIES OF WFS AND HOA

The comparison of WFS and HOA is performed in several steps. The physical properties will be investigated first. Then a closer look is taken at the driving functions and the resulting reproduced wave fields.

5.1. Physical Properties

The physical properties of both approaches are given by the underlying basic theory, as presented in Section 2, and the particular derivation of the algorithms, as presented in Section 3. The resulting properties will be discussed in the following. The influence of spatial sampling will be investigated in the next sections.

HOA is based on an explicit solution of a simple source formulation. The simple source formulation constitutes a boundary integral equation of the first kind. It is known from the underlying mathematics that the solution is potentially not unique and ill-posed. The non-uniqueness doesn't allow to control the wave field within the listening area at some distinct frequencies, while the ill-posedness implies numerical problems for the calculation of the driving function. HOA has numerical problems due to ill-posedness of the driving function. This can be concluded from (13). Due to the zeros of the Bessel function, the numerator and denominator is zero at some frequencies. Depending on the properties of the numerator numerical problems may arise when computing the driving function at some distinct frequencies. Standard regularization techniques can be applied in order to overcome this problem. Both the non-uniqueness and the ill-posedness occur typically only at a limited number of discrete frequencies. Outside of these frequencies, the reproduced wave field matches exactly the desired one within the entire listening area. The explicit form of the driving function for HOA depends on the underlying geometry of the problem. Currently solutions exist for circular/spherical secondary source contours.

The theoretical foundation of WFS is based on a Neumann Green's function describing the wave field of the secondary sources. WFS applies the Neumann Green's function for a linear/planar boundary ∂V, since such secondary sources are in general impossible to realize for arbitrary secondary source contours. This function can be realized by monopole secondary sources. The wave field reproduced by WFS is only exact for linear/planar secondary source contours, as a consequence. The extension to arbitrarily shaped convex secondary source contours is performed by sensibly selecting the active secondary sources. For a circular secondary source contour, the reproduced wave field will exhibit inaccuracies due to the wrong type of secondary sources. This holds also for other non-linear/-planar geometries. However, these inaccuracies seem to be of minor relevance in practical implementations (see e. g. Fig. 6(a)). WFS doesn't seem to suffer from non-uniqueness or ill-posedness problems in typical situations. This is due to the fact that not all secondary sources are use to reproduce a particular wave field and hence no resonances occur. Furthermore, the secondary source driving function, as given by (14), exhibits no ill-posedness.

Note, that for both approaches a wave field is also reproduced outside of the listening area, contrary to the Kirchhoff-Helmholtz integral.

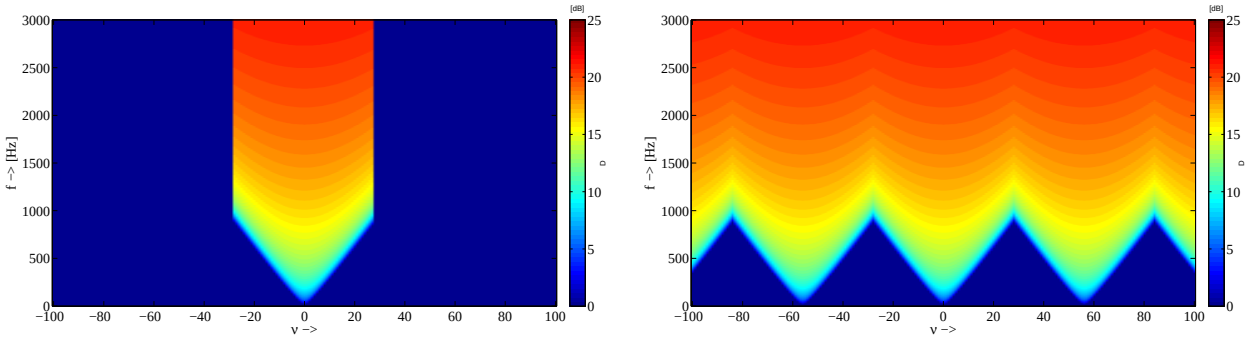

(a) continuous (b) sampled

Fig. 3: Absolute value $\left|\mathring{D}_{\mathrm{HOA}}(\nu, R, \omega)\right|$ of the angular spectrum of the HOA driving function for a virtual plane wave.

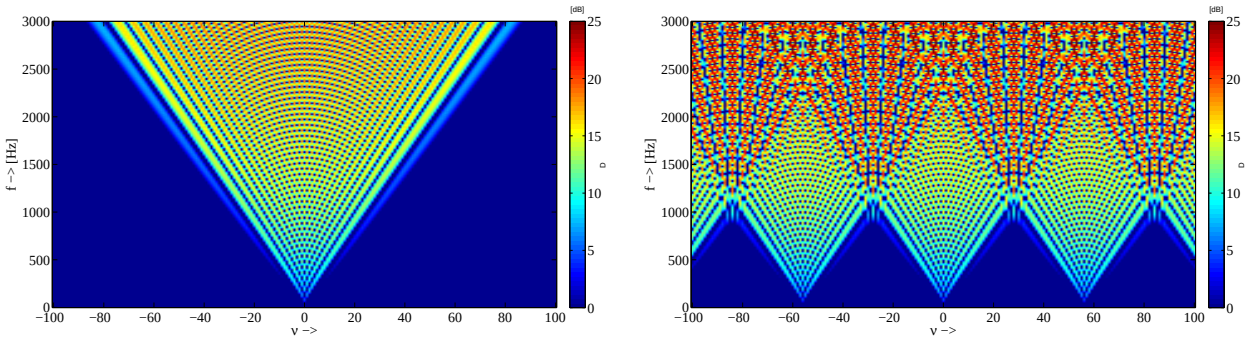

(a) continuous (b) sampled

Fig. 4: Absolute value $\left|\mathring{D}_{\mathrm{WFS}}(\nu, R, \omega)\right|$ of the angular spectrum of the WFS driving function for a virtual plane wave.

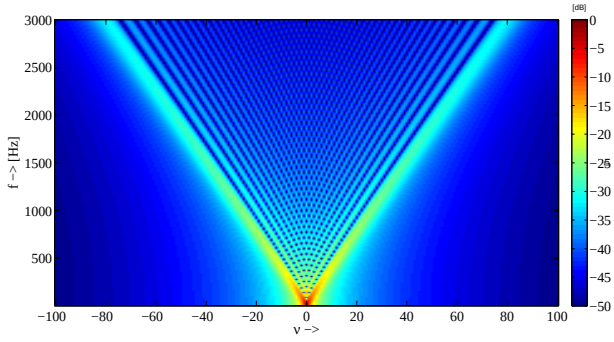

Fig. 5: Absolute value of the angular spectrum of a secondary line source.

5.2. Driving Functions

The following sections illustrate the different properties of WFS and HOA using a numerical simulation of both systems. For this purpose, a circular reproduction system with a radius of $R = 1.50$ m consisting of $N = 56$ secondary monopole line sources was simulated. The driving functions for both approaches where calculated for a plane wave as desired virtual wave field. Depending on the investigation, the plane wave is either assumed to be monochromatic or a bandlimited Dirac pulse. The incidence angle of the plane wave is $\theta_{\mathrm{pw}} = 270^{\mathrm{o}}$ for all simulations. For the situations shown in the various figures, the plane wave travels parallel to the y-axis from top to down. The angular bandwidth of the HOA driving signal is bandlimited according to (16).

Figure 3 depicts the angular spectrum $\mathring{D}_{\mathrm{HOA}}(\nu, R, \omega)$ of the continuous and sampled HOA driving function. The band-limitation of the driving function can be seen clearly in Fig. 3(a), the spectral repetitions due to angular sampling in Fig. 3(b). Note, that no spectral overlaps are present in the latter figure due to the band-limitation of the HOA driving function.

Figure 4 shows the angular spectrum $\mathring{D}_{\mathrm{WFS}}(\nu, R, \omega)$ of the continuous and sampled WFS driving function. Figure 4(a) reveals that the driving function for WFS is not band-limited in the angular frequency domain. Consequently, this leads to spectral overlaps and aliasing when the driving function is sampled, as can be seen in Fig. 4(b).

It can be deduced from Fig. 3 and 4 that both driving functions exhibit spectral repetitions due to angular sampling. However, due to the missing band-limitation for WFS, in this case the sampled driving function contains aliasing. According to Eq. (12), the reproduction of the spectral repetitions in the driving function depends on the angular spectrum of the secondary sources. If the secondary sources resemble an ideal low-pass then none of these repetitions are reproduced. However, the characteristics of the angular spectrum are given by the actual type of secondary sources used. Figure 5 depicts the angular spectrum of a line source. It is evident that the spectrum is not band-limited. Hence, the spectral repetitions present in the driving functions of WFS and HOA will be reproduced to some extend.

5.3. Reproduction of Monochromatic Plane Waves

Figures 6 and 7 show the reproduced wave field for a monochromatic virtual plane wave with varying frequency f_{pw}. The left rows show WFS, the right rows HOA. According to Fig. 6(b), HOA provides accurate reproduction within the listening area for the lowest frequency shown ($f_{\mathrm{pw}} = 500$). For WFS some slight deviations from the desired plane wave are visible at the lower end of the listening area close to the secondary sources (see Fig. 6(a)). These deviations are due to the fact that the secondary sources do not match the wave field of the required Neumann Green's function for that situation. As the frequency of the plane wave increases, also the reproduced wave fields of WFS and HOA show an increasingly amount of artifacts. For instance, in Fig. 6(e) strong interferences can be observed in the upper part of the listening area. These constitute spatial aliasing due to spectral overlaps in the driving function for WFS. It can be seen in Fig. 6(f) for HOA, that the area where the reproduced wave field matches the desired plane wave is approximately a circular region around the center of the listening area. Outside of this area strong sampling artifacts occur. However, these artifacts look quite different than for WFS.

Hence, the spatial structure of the sampling artifacts for WFS and HOA differ significantly. This can be observed more clearly in Fig. 7(e) and Fig. 7(f). While the spatial aliasing artifacts for WFS are less pronounced with an increasing distance of the listener to the active secondary sources, the reproduction error of HOA is minimal in the center of the listening area. Furthermore, the artifacts for WFS are quite unstructured, while these are much more structured for HOA. Especially in Fig. 7(f), the artifacts on the sides constitute approximately plane waves which are tilted towards the upmost loudspeakers. This could imply, that these loudspeakers can be localized quite well by the listeners. Further investigation of the angular energy distribution of the driving function supports this observation. Almost all energy in the driving function is assigned to the upmost loudspeaker for higher frequencies. For WFS this is not the case. For HOA, also the level of the sampling artifacts varies strongly with frequency and to some lesser extend with the position. This could imply strong colorations for listener positions

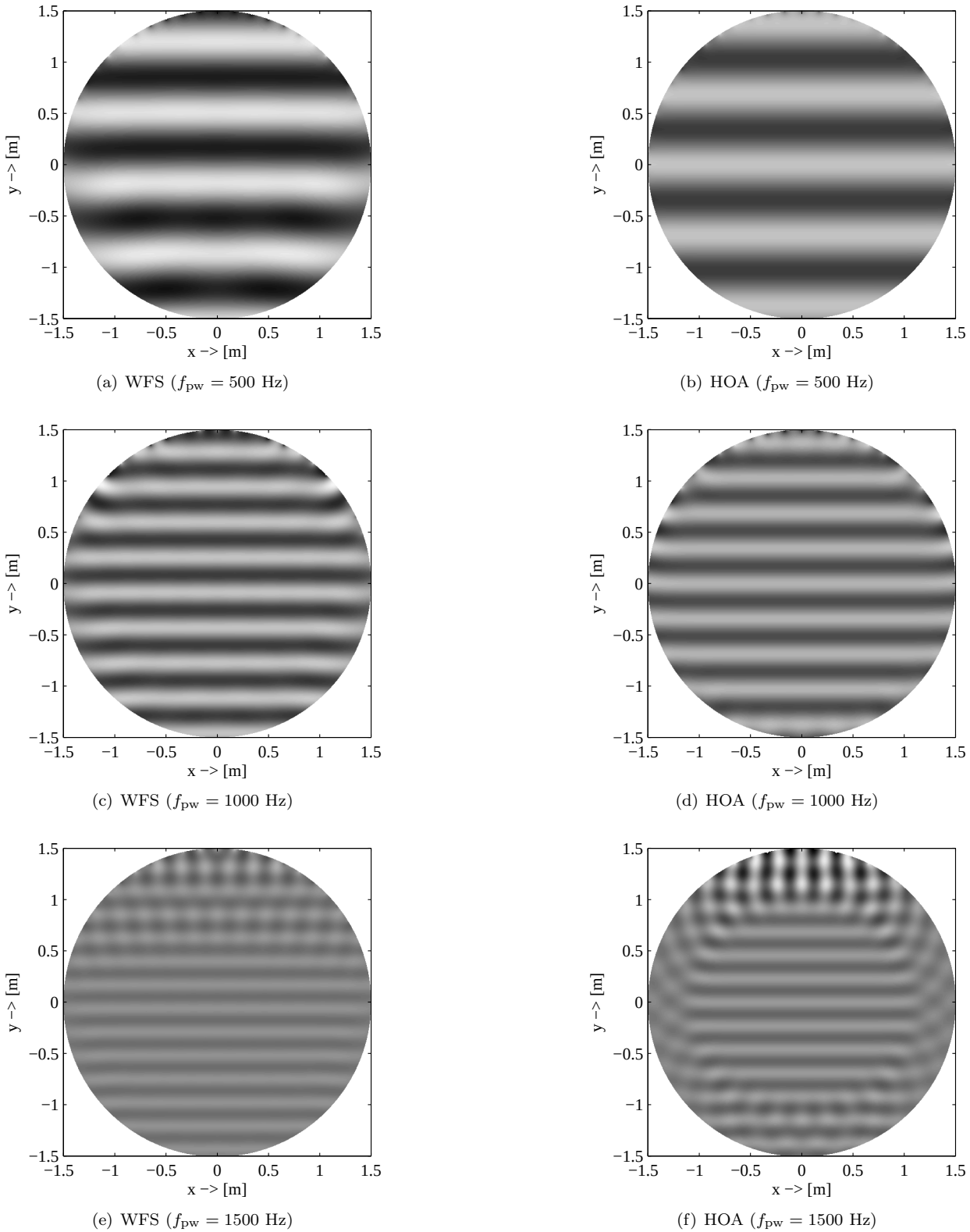

(a) WFS ($f_{\mathrm{pw}} = 500$ Hz)

(b) HOA ($f_{\mathrm{pw}} = 500$ Hz)

(c) WFS ($f_{\mathrm{pw}} = 1000$ Hz)

(d) HOA ($f_{\mathrm{pw}} = 1000$ Hz)

(e) WFS ($f_{\mathrm{pw}} = 1500$ Hz)

(f) HOA ($f_{\mathrm{pw}} = 1500$ Hz)

Fig. 6: Reproduced wave field for a monochromatic virtual plane wave.

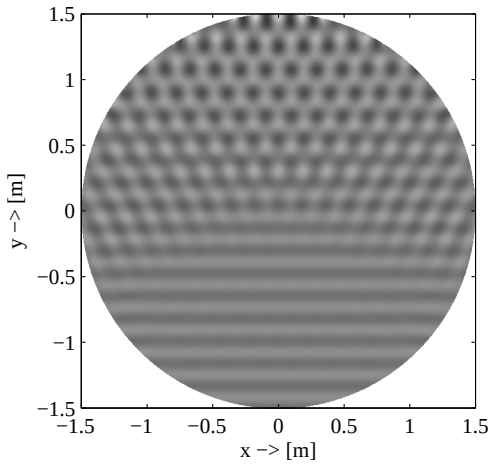

(a) WFS ($f_{\mathrm{pw}} = 2000$ Hz)

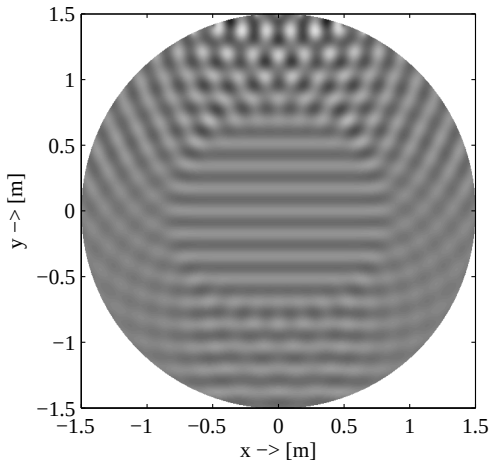

(b) HOA ($f_{\mathrm{pw}} = 2000$ Hz)

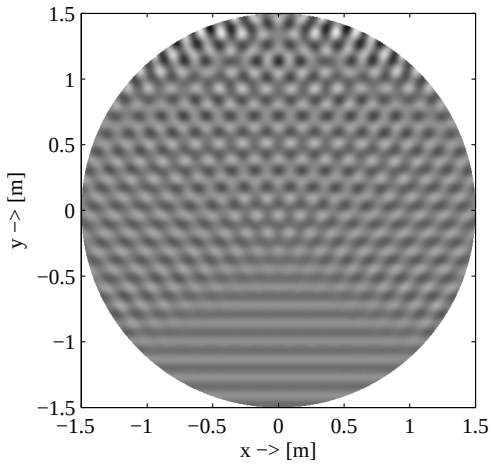

(c) WFS ($f_{\mathrm{pw}} = 2500$ Hz)

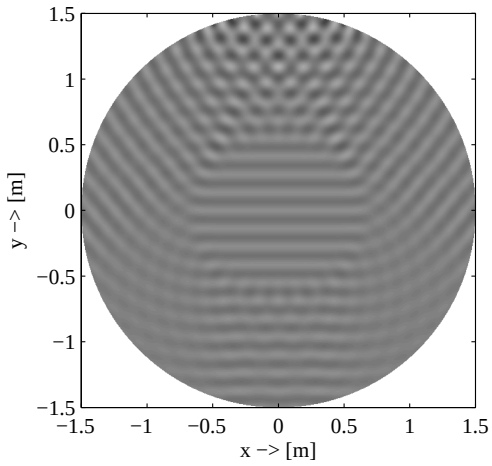

(d) HOA ($f_{\mathrm{pw}} = 2500$ Hz)

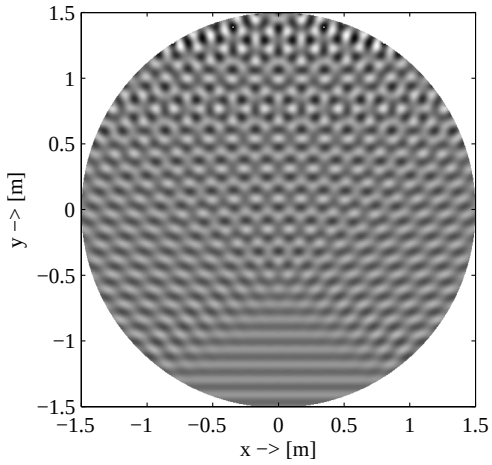

(e) WFS ($f_{\mathrm{pw}} = 3000$ Hz)

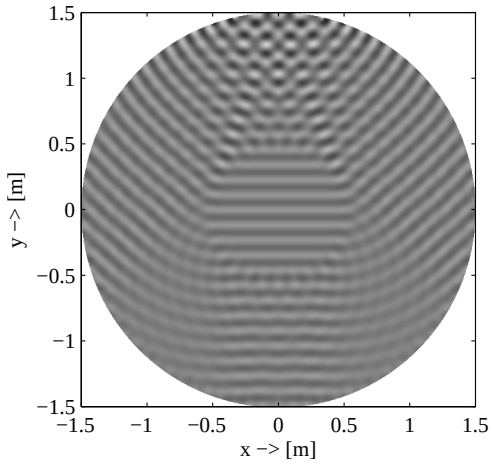

(f) HOA ($f_{\mathrm{pw}} = 3000$ Hz)

Fig. 7: Reproduced wave field for a monochromatic virtual plane wave.

outside of the center in HOA.
For both WFS and HOA, this downsizing of the area where the desired wave field is reproduced correctly continues as the frequency increases further.

5.4. Reproduced Aliasing to Signal Ratio

In order to analyze the reproduction errors in a more quantitative fashion, the RASR was computed for a band-limited plane wave with varying bandwidth b_{pw}. The results are illustrated in Figures 8 and 9. The findings from the previous section, with respect to the spatial structure of the spatial sampling artifacts, are confirmed clearly. It can be seen additionally that for HOA, similar to WFS, the sampling artifacts are less pronounced for listeners in the lower part of the listening area. This is due to the fact that the upper loudspeakers are the ones driven with the highest levels. For both, WFS and HOA, the overall size of the almost artifact free reproduction area is quite similar. However, HOA has the advantage that this area is located at a fixed position. Only the size varies here. For the highest bandwidth shown here this circular region has a diameter of about 1 m. In order to be able to reproduce the wave field accurately around the head of one listener, this region should be at least 30 cm in diameter. Further simulations revealed that the reproduction of a plane wave with a frequency up to 10 kHz is possible just around the head of one listener without severe sampling artifacts.
Its also interesting to note, that the energy of the aliasing contributions increases in a quite steep fashion.

6. CONCLUSION

This paper presents a comparison of two massive multichannel sound reproduction techniques, namely WFS and HOA. We started off with a formulation of both approaches in a common framework which included their underlying physical basis and the realization by a spatially discrete distribution of secondary sources. This mathematical view was complemented by numerical simulations of the reproduced wave fields. The results presented in this paper revealed a number of differences between WFS and HOA. Some of the differences between both approaches that have been reported in the literature where confirmed. However, also a number of new findings could be derived.
The main findings for WFS are: (1) it provides an explicit formulation of the driving function for arbitrary convex secondary source contours, (2) the computations of the driving signals can be realized quite cheaply, (3) even when discarding spatial sampling, the desired wave field is not reproduced exactly within the listening area for curved secondary source contours, (4) the area with almost sampling artifact-free reproduction is not at a constant position, (5) the sampling artifacts exhibit irregular structures and (6) are potentially perceived as coloration of the virtual source [22].
The main findings for HOA are: (1) explicit formulations of the driving function can only be derived by considering a particular geometry, (2) the computation of the driving signals might become quite complex due to the special functions involved, (3) exact reproduction within the listening area is in principle possible, (4) almost sampling artifact-free reproduction is possible in a circular region around the listening area, (5) the sampling artifacts exhibit quite regular structures, (6) the sampling artifacts may give rise to strong coloration of the virtual source and (7) HOA potentially suffers from non-uniqueness and ill-conditioning.
These results show that WFS and HOA are not similar even when discarding spatial sampling and that the sampling artifacts of both approaches differ significantly from each other. Sound reproduction systems are mainly designed for human listeners and hence their perceptual difference is of major interest. The differences between WFS and HOA derived in this paper are based on mathematical formulations and numerical simulations. Their psychoacoustic impact is not clear at the current stage. However, the results might give some indications. For instance, the structure of the sampling artifacts for HOA indicates that listeners perceive the sound as coming from one distinct position on the secondary source contour for the reproduction of a plane wave. This effect was already observed in a first informal listening test. More work has to be performed for a subjective comparison of both approaches. The work presented in this paper may lay the ground for the design of these experiments.

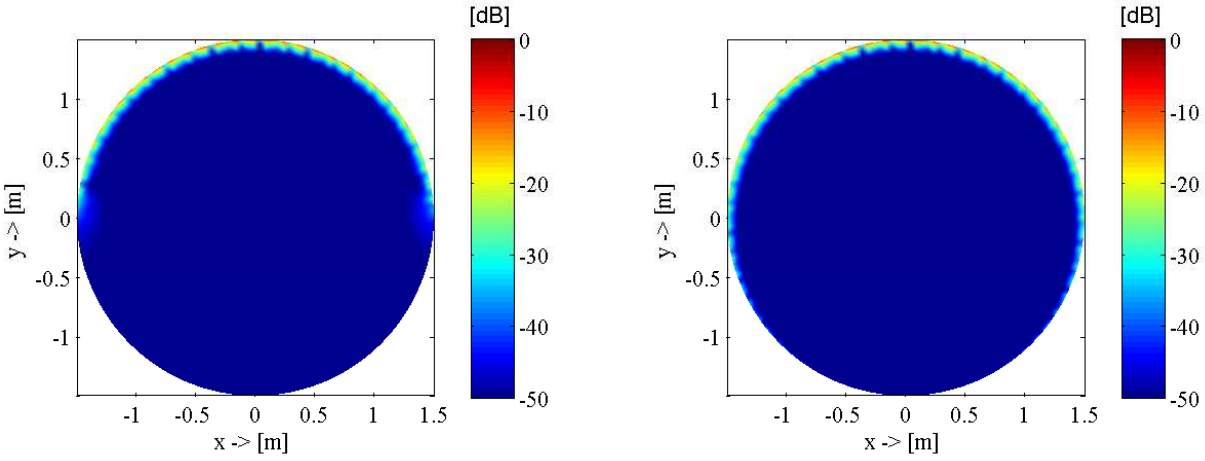

(a) WFS ($b_{\mathrm{pw}} = 500$ Hz)

(b) HOA ($b_{\mathrm{pw}} = 500$ Hz)

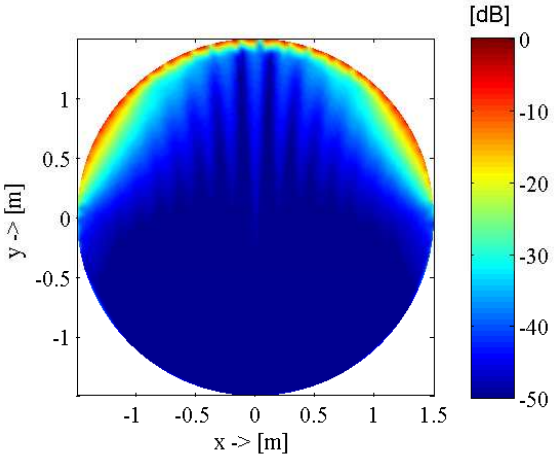

(c) WFS ($b_{\mathrm{pw}} = 1000$ Hz)

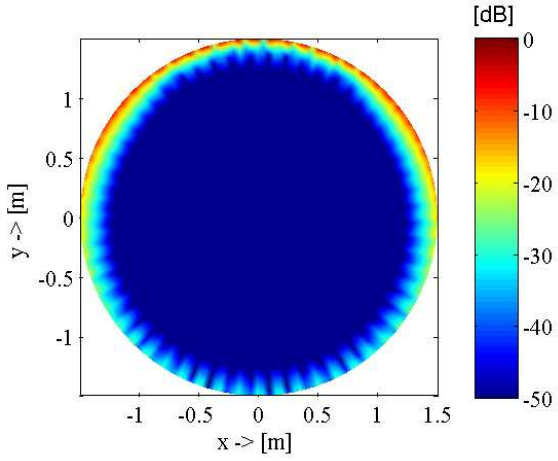

(d) HOA ($b_{\mathrm{pw}} = 1000$ Hz)

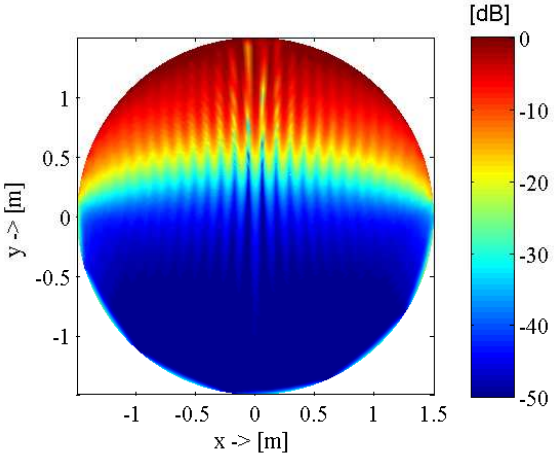

(e) WFS ($b_{\mathrm{pw}} = 1500$ Hz)

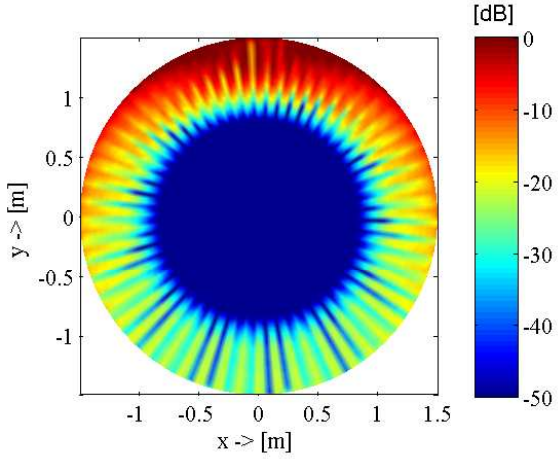

(f) HOA ($b_{\mathrm{pw}} = 1500$ Hz)

Fig. 8: Reproduced aliasing to signal ratio $\mathrm{RASR}(\mathbf{x}, b_{\mathrm{pw}})$ for a bandlimited virtual plane wave.

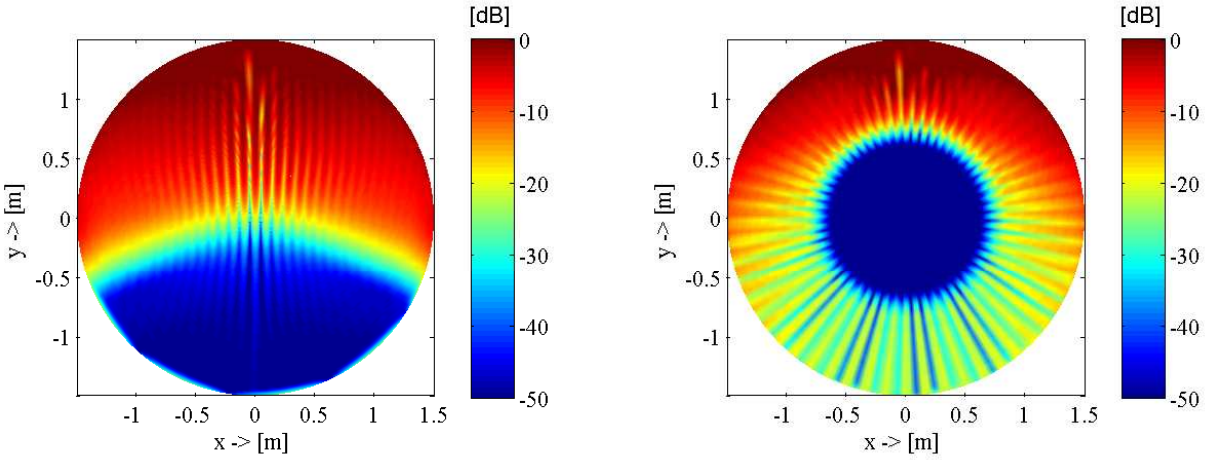

(a) WFS ($b_{\mathrm{pw}} = 2000$ Hz)

(b) HOA ($b_{\mathrm{pw}} = 2000$ Hz)

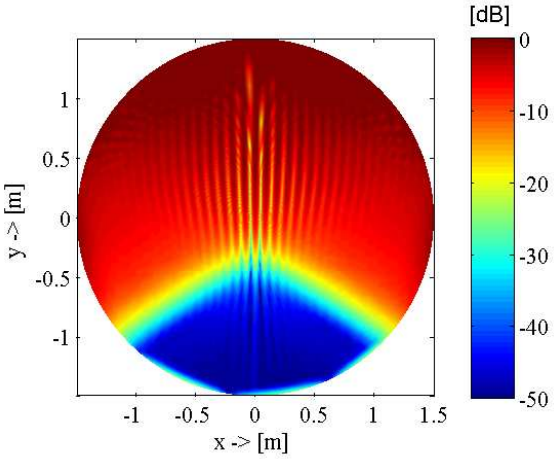

(c) WFS ($b_{\mathrm{pw}} = 2500$ Hz)

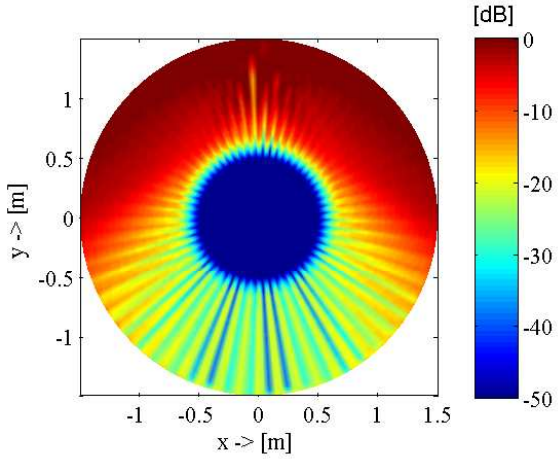

(d) HOA ($b_{\mathrm{pw}} = 2500$ Hz)

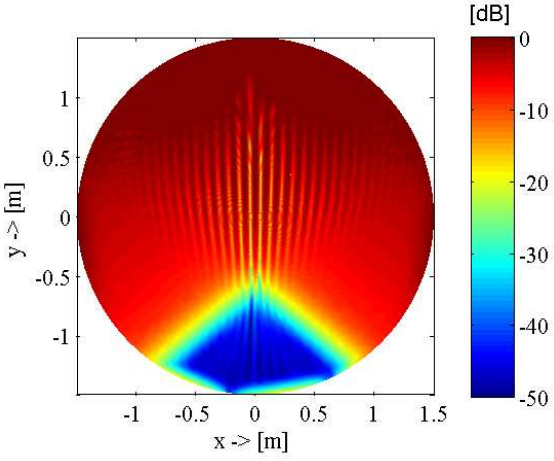

(e) WFS ($b_{\mathrm{pw}} = 3000$ Hz)

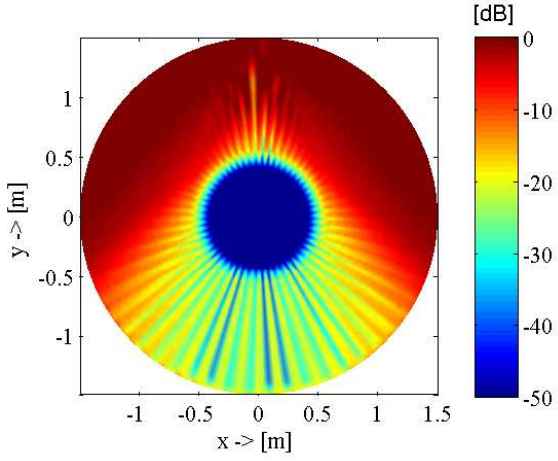

(f) HOA ($b_{\mathrm{pw}} = 3000$ Hz)

Fig. 9: Reproduced aliasing to signal ratio $\mathrm{RASR}(\mathbf{x}, b_{\mathrm{pw}})$ for a bandlimited virtual plane wave.

7. REFERENCES

[1] A.J. Berkhout. A holographic approach to acoustic control. *Journal of the Audio Engineering Society*, 36:977–995, December 1988.

[2] M.A. Gerzon. With-heigth sound reproduction. *Journal of the Audio Engineering Society (JAES)*, 21:2–10, 1973.

[3] J. Daniel. *Représentation de champs acoustiques, application à la transmission et à la reproduction de scènes sonores complexes dans un contexte multimédia*. PhD thesis, Université Paris 6, 2000.

[4] J. Daniel. Spatial sound encoding including near field effect: Introducing distance coding filters and a viable, new ambisonic format. In *AES 23rd International Conference*, Copenhagen, Denmark, May 2003. Audio Engineering Society (AES).

[5] J. Daniel, R. Nicol, and S. Moreau. Further investigations of high order ambisonics and wavefield synthesis for holophonic sound imaging. In *114th AES Convention*, Amsterdam, The Netherlands, March 2003. Audio Engineering Society (AES).

[6] R. Nicol and M. Emerit. Reproducing 3D-sound for videoconferencing: A comparison between holophony and ambisonic. In *First COST-G6 Workshop on Digital Audio Effects (DAFX98)*, Barcelona, Spain, Nov. 1998.

[7] S. Spors. Comparison of higher-order ambisonics and wave field synthesis with respect to spatial aliasing artifacts. In *19th International Congress on Acoustics*, Madrid, Spain, September 2007.

[8] E.G. Williams. *Fourier Acoustics: Sound Radiation and Nearfield Acoustical Holography*. Academic Press, 1999.

[9] P.M. Morse and H. Feshbach. *Methods of theoretical physics. Part II*. McGraw-Hill, New York, 1953.

[10] L.G. Copley. Fundamental results concerning integral representations in acoustic radiation. *Journal of the Acoustical Society of America*, 44(1):28–32, 1968.

[11] J. Giroire. Integral equation methods for the helmholtz equation. *Integral Equations and Operator Theory*, 5(1):506–517, 1982.

[12] J. Ahrens and S. Spors. Analytical driving functions for higher-order ambisonics. In *IEEE International Conference on Acoustics, Speech, and Signal Processing (ICASSP)*, April 2008.

[13] J. Ahrens and S. Spors. An analytical approach to sound field reproduction using circular and spherical loudspeaker distributions. *Acta Acoustica united with Acoustica*, 2008. To appear.

[14] M.A. Poletti. Three-dimensional surround sound systems based on spherical harmonics. *Journal of the AES*, 53(11):1004–1025, November 2005.

[15] Y.J. Wu and T. Abhayapala. Soundfield reproduction using theoretical continous loudspeaker. In *IEEE International Conference on Acoustics, Speech, and Signal Processing (ICASSP)*, Las Vegas, USA, 2008.

[16] S. Spors, R. Rabenstein, and J. Ahrens. The theory of wave field synthesis revisited. In *124th AES Convention*, Amsterdam, The Netherlands, May 2008. Audio Engineering Society (AES).

[17] S. Spors. Extension of an analytic secondary source selection criterion for wave field synthesis. In *123th AES Convention*, New York, USA, October 2007. Audio Engineering Society (AES).

[18] J.-J. Sonke, D. de Vries, and J. Labeeuw. Variable acoustics by wave field synthesis: A closer look at amplitude effects. In *104th AES Convention*, Amsterdam, Netherlands, May 1998. Audio Engineering Society (AES).

[19] S. Spors and R. Rabenstein. Spatial aliasing artifacts produced by linear and circular loudspeaker arrays used for wave field synthesis. In *120th AES Convention*, Paris, France, May 2006. Audio Engineering Society (AES).

[20] M. Abramowitz and I.A. Stegun. *Handbook of Mathematical Functions*. Dover Publications, 1972.

[21] P.M. Morse and H. Feshbach. *Methods of theoretical physics. Part I.* McGraw-Hill, New York, 1953.

[22] H. Wittek. *Perceptual differences between wavefield synthesis and stereophony.* PhD thesis, University of Surrey, 2007.